Mechanistic Studies of a New Nucleated Infectious Development System Using Pyridinium Salts: Nucleation of Silver Halide Grains by Dihydropyridines

Naoki Obi*, Jun Takeuchi, Yasuhiko Kojima, and Yasuo Shigemitsu‡

Dainippon Ink & Chemicals, Inc., 3-35-58, Sakashita, Itabashi-ku, Tokyo 174, Japan

A. Gary DiFrancesco* and Richard K. Hailstone†

Center for Imaging Science, Rochester Institute of Technology, 54 Lomb Memorial Drive, Rochester, New York 14623-5604

Photographic properties of 1-benzyl-1,4-dihydronicotinamide (BNAH) are studied for better understanding of the mechanism of the production of high contrast by the infectious development induced by the combination of a pyridinium salt and Metol-ascorbate developer. Treatment of silver bromide emulsion or silver chlorobromo emulsion by BNAH and redox buffer followed by development gave high fog density. It has been suggested that the oxidation product of BNAH by redox buffer nucleates silver halide grains and makes them developable. Results support the hypothesis that dihydropyridine works as an intermediate in the production of high contrast by the infectious development in the presence of a pyridinium salt.

Journal of Imaging Science and Technology 42: 221–227 (1998)

Introduction

High-contrast photographic materials are used for line and halftone works in the graphic arts industry. Contrast of the films used for cameras and imagesetters are typically greater than 15 with the maximum density of greater than 4. Special technologies are needed to obtain such a high contrast with high maximum density. Currently, hydrazide nucleation technology is widely accepted in the graphic arts industry to design a high-contrast system because hydrazide nucleation technology provides not only good image quality but also rapid processing.

We recently found that a pyridinium salt works as a nucleator to give superhigh contrast.[1] This finding was applied to design a new hybrid system that provides both superhigh contrast (greater than 15 between densities 0.5 and 3.0 above base plus fog) and rapid access developability for the graphic arts industry.

The new hybrid system by a pyridinium salt is an environmentally improved system and has the following unique features: The system does not use any hydroquinone as a developing agent but uses ascorbic acid as a main developing agent. Pyridinium nucleation system works with lower pH than the hydrazide nucleation system, and the pH of the developer for the model hybrid system is 9.8. The system does not uses an amine compound called booster required in the hydrazide hybrid system. Design of a new electron accepting nucleating agent succeeded in obtaining a direct-positive superhigh-contrast image.[2]

The nucleation reaction by a pyridinium salt is of great interest not only because of the unique characteristics mentioned above but also because hydrazine or its derivatives, hydrazides, currently are the only nucleators to obtain high contrast. Results of mechanistic study using 1-benzyl-3-carbamoylpyridinium salt (BNA^+) and 1-benzyl-1,4-dihydronicotinamide (BNAH) (structures of BNA^+ and BNAH are shown in Fig. 1) in the negative emulsion system suggest that the increase of contrast and apparent photographic speed is due to the image-wise nucleation of silver halide grains by active species derived from BNAH which is the two electron reduced form of BNA^+. The following mechanism has been proposed[1] to account for the production of superhigh contrast in the presence of 1-benzyl-3-carbamoylpyridinium salt (BNA^+):

$$AgX(Ag^0) + M \rightarrow Ag^0{}_n + Mox, \quad (1)$$

$$Mox + AA \rightarrow M + AAox, \quad (2)$$

$$BNA^+ + M\ (or\ AA) \xrightarrow{2e^-,H^+} BNAH + Mox\ (or\ AAox), \quad (3)$$

$$BNAH + Mox \rightarrow Nu, \quad (4)$$

Original manuscript received April, 28, 1997

* IS&T Member

† IS&T Fellow

‡ Current affiliation; Kawamura Institute of Chemical Research, 631, Sakado, Sakura-shi, Chiba-ken 285, Japan

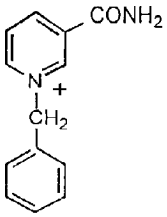

1-Benzyl-3-carbamoyl-pyridinium salt (BNA^+)

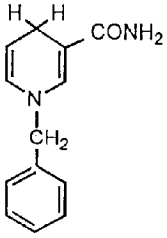

1-Benzyl-1,4-dihydronicotinamide (BNAH)

Figure 1. Structures of 1-benzyl-3-carbamoylpyridinium salt (BNA^+) and 1-benzyl-1,4-dihydronicotinamide (BNAH).

$$AgX + Nu \rightarrow AgX(Ag^0) + Nuox, \quad (5)$$

$$AgX(Ag^0) + M \rightarrow Ag^0{}_n + Mox, \quad (6)$$

where

AgX	=	unexposed silver halide
$AgX(Ag^0)$	=	exposed or nucleated silver halide
$Ag^0{}_n$	=	developed silver
M	=	Metol
Mox	=	oxidized form of Metol
AA	=	ascorbate
$AAox$	=	oxidized form of ascorbate
Nu	=	active species for nucleation.

It has been assumed that a dihydropyridine is an intermediate of the nucleation reaction and that the oxidation product of dihydropyridine is a possible active species for the nucleation of silver halide grains. Preliminary results showed that prebath treatment of a film sample by BNAH and potassium ferricyanide before development is a useful method to study the photographic effect of BNAH and indicated that the reaction product of BNAH and ferricyanide is capable to nucleate unsensitized AgClBr grains.[3] In this article we report further study of the prebath treatment of silver halide emulsion by BNAH and ferricyanide.

Experimental

Oxidation of BNAH by Ferricyanide. UV spectra of a solution containing 0.05 mM BNAH and 0.20 mM $K_3Fe(CN)_6$ was measured to study the reaction between BNAH and $K_3Fe^{III}(CN)_6$. BNAH methanol solution (0.25 mM) and 0.25 M $NaBO_2 \bullet 4H_2O$ solution containing 0.25 mM $K_3Fe(CN)_6$ (pH 9.8) were mixed at a ratio of 1:4 (v/v). Concentrations of BNAH and $K_3Fe(CN)_6$ after the mixing were 0.05 and 0.20 mM, respectively. The UV spectra were measured at 23°C on a UV-VIS recording spectrophotometer (Shimazu Corporation, Kyoto, Japan).

Emulsion. A monodispersed cubic AgClBr emulsion having a mean edge length of 0.18 μm (Cl/Br = 70/30) and a monodispersed octahedral AgBr emulsion having a mean edge length of 0.47 μm were used in this study. Both emulsions were prepared by a controlled double-jet method. The AgClBr emulsion was coated on a PET base without chemical sensitization. Coating weight was 40 mgAg/dm^2. The AgBr emulsion was used with and without chemical sensitization. Film samples with different photographic speeds were prepared to study the effect of photographic speed on the nucleation. Chemical sensitization was performed by adding sodium thiosulfate pentahydrate to the emulsion, and five different amounts of sodium thiosulfate pentahydrate, 2.6, 4.0, 5.4, 6.7, and 8.1×10^{-6} mol/molAg, were used to change the photographic speed. After the addition of sodium thiosulfate pentahydrate, the emulsion was digested at 70°C for 40 min. The emulsions were then coated on a PET base. Coating weight was 22 mgAg/dm^2.

TABLE I. Standard Solutions for Nucleation Test (AgClBr Emulsion)

BNAH solution	0.25 M $NaBO_2 \cdot 4H_2O$ aqueous solution containing 1 mM BNAH (pH 9.8)
Redox solution	0.25 M $NaBO_2 \cdot 4H_2O$ aqueous solution containing 1.4 mM $K_3Fe^{III}(CN)_6$ (pH 9.8)
Developer	Kodak D19

TABLE II. Standard Solutions for Nucleation Test (AgBr Emulsion)

BNAH solution	0.25 M $NaBO_2 \cdot 4H_2O$ aqueous solution containing 2.5×10^{-5} M BNAH (pH 9.8)
Redox solution	0.25 M $NaBO_2 \cdot 4H_2O$ solution containing $K_4Fe^{II}(CN)_6/K_3Fe^{III}(CN)_6$ = 4 mM/1 mM (pH 9.8)
Developer	Kodak D19

Nucleation Experiment. An experiment to model the nucleation of silver halide grains by the oxidation product of BNAH was designed as follows. An unexposed film sample was soaked in a BNAH solution and was then soaked in a redox solution containing $K_4Fe^{II}(CN)_6$ and/or $K_3Fe^{III}(CN)_6$. No washing was done between BNAH solution and redox solution treatment, allowing that BNAH would react with the redox couple in the redox solution. The film sample was then subjected to development. Fog density was measured after treating the film sample with a stop and a fix. Tables I and II summarize the solutions used for the nucleation test.

Sensitometric Experiments. AgBr film samples were exposed by a EG&G Mark VII sensitometer for 10^{-2} s through a 0.15 log H increment step wedge. Exposed films were developed with Kodak D19 developer (Rochester, New York) at 20°C, followed by a stop and a fix. Photographic speed was measured at D=1.6 above base plus fog.

Measurement of Redox Potential of Redox Buffer. Redox potential of the redox buffer was measured with an IBM EC225 Voltammetric Analyzer. The working electrode and counter electrode were platinum wire. The reference electrode was a saturated calomel electrode (SCE).

Results

Oxidation of BNAH by $Fe^{III}(CN)_6^{3-}$. Figure 2 shows the UV spectral change of the solution containing 0.05 mM BNAH and 0.20 mM $K_3Fe(CN)_6$. With increasing reaction time, the absorption maximum assigned to BNAH (360 nm) and $Fe^{III}(CN)_6^{3-}$ (304 and 423 nm) decreased, while the absorption maximum for $Fe^{II}(CN)_6^{4-}$ (260 nm) increased. Results in Fig. 2 suggested that BNAH reduced $Fe^{III}(CN)_6^{3-}$

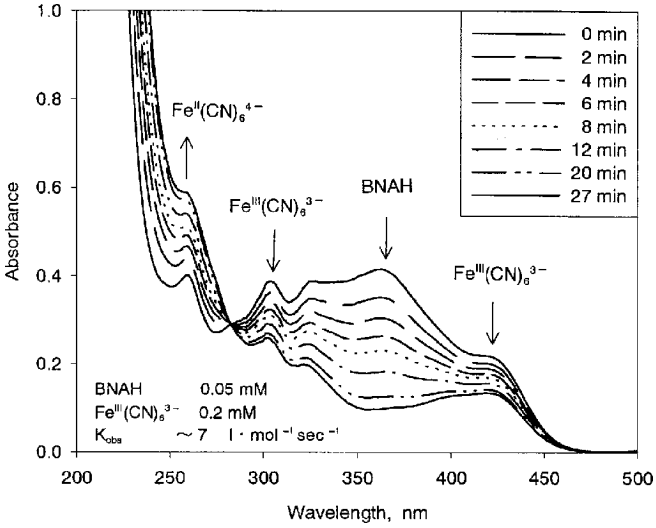

Figure 2. UV spectral change of a mixture of BNAH and $K_3Fe^{III}(CN)_6$ solutions.

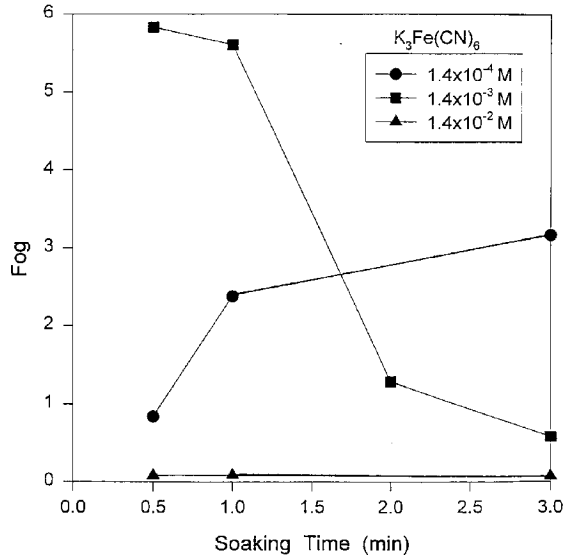

Figure 3. Dependence of fog density on the soaking time in various concentrations of $K_3Fe^{III}(CN)_6$ solution (AgClBr emulsion).

TABLE III. Treatment Conditions and Results (AgClBr Emulsion)*

Sample	Process	Fog density
1	Development by D19 only	0.05
2	Film sample was soaked in BNAH solution, and then developed by D19	0.05
3	Film sample was soaked in BNAH solution, in redox solution (1.4 mM $K_3Fe^{III}(CN)_6$ solution), and then developed by D19	5.4
4	Film sample was soaked in BNAH solution, in redox solution (1.4 mM $K_4Fe^{II}(CN)_6$ solution)†, and then developed by D19	0.05

* Treatment time was 1min at 30°C for all the solutions. After development, film samples were treated in a stop bath and were then fixed.
† Note that 1.4 mM $K_4Fe^{II}(CN)_6$ solution was used instead of 1.4 mM $K_3Fe^{III}(CN)_6$ solution.

to produce $Fe^{II}(CN)_6^{4-}$. The observed rate constant was 7 M^{-1} s^{-1} (second order).

Fog Increase by BNAH and Redox Solution Treatment. An unexposed AgClBr film sample was treated using the solutions listed in Table I. The conditions of treatment and fog density observed for each film sample are summarized in Table III. As shown in Table III, high fog density was observed when the film sample was treated by 1 mM BNAH solution and 1.4 mM $K_3Fe^{III}(CN)_6$ solution before the development by D19 (Sample 3). When treatment by $K_3Fe^{III}(CN)_6$ solution was omitted and the film sample was treated by BNAH followed by development (Sample 2), the fog density was 0.05 and was the same as the base plus fog density obtained by development without any treatment. Sample 4 was treated by the same procedure as Sample 3 except that 1.4 mM $K_4Fe^{II}(CN)_6$ solution was used as a redox solution instead of 1.4 mM $K_3Fe^{III}(CN)_6$ solution. Unlike the case of Sample 3, fog density obtained was 0.05 and no increase of fog density occured.

Figure 3 shows dependence of fog density on soaking time in various concentrations of $K_3Fe^{III}(CN)_6$. Conditions other than the concentration of the $K_3Fe^{III}(CN)_6$ solution and its treatment time were the same as Sample 3 in Table III. It is shown that fog density strongly depends on $K_3Fe^{III}(CN)_6$ concentration and treatment time in a $K_3Fe^{III}(CN)_6$ solution. When the concentration of $K_3Fe^{III}(CN)_6$ solution was 1.4×10^{-3} M (standard concentration), fog density decreased rapidly with increased treatment time of $K_3Fe^{III}(CN)_6$ solution in the range of treatment times tested in this experiment. But, when the concentration of $K_3Fe^{III}(CN)_6$ solution was 1.4×10^{-4} M, fog density increased with increasing treatment time of $K_3Fe^{III}(CN)_6$ solution. When the concentration of $K_3Fe^{III}(CN)_6$ solution was 1.4×10^{-2} M, fog density was 0.04 and no fog increase was observed.

TABLE IV. Treatment Conditions and Results (Unsensitized AgBr Emulsion)*

Sample	Process	Fog Density
1	Development by D19 only	0.04
2	Film was soaked in BNAH solution and then developed by D19	0.07
3	Film was soaked in BNAH solution, in redox solution ($K_4Fe^{II}(CN)_6/K_3Fe^{III}(CN)_6$ = 4 mM/1 mM solution), and then developed by D19	0.94
4	Film was soaked in BNAH solution, in redox solution (5 mM $K_4Fe^{II}(CN)_6$ solution)†, and then developed by D19	0.04

* Treatment time was 1 min for BNAH solution, 30 s for redox solution, 12 min for development. Treatment temperature was 20°C for all solutions.
† Note that 5 mM $K_4Fe^{II}(CN)_6$ solution was used instead of $K_4Fe^{II}(CN)_6/K_3Fe^{III}(CN)_6$ = 4 mM/1 mM solution.

Similar experiments were performed using unexposed an octahedral AgBr emulsion. Solutions used for the AgBr emulsion are shown in Table II. Concentration of BNAH was lowered to 2.5×10^{-5} M from 1×10^{-3} M used for AgClBr. A mixture of $K_4Fe^{II}(CN)_6$ and $K_3Fe^{III}(CN)_6$ was used as a redox solution instead of $K_3Fe^{III}(CN)_6$ alone to study the effect of redox potential of the redox solution on fog density. Temperature of the treatment was lowered to 20°C from 30°C. As shown in Table IV, similar results to AgClBr were obtained. High fog density was observed when the film sample was treated by BNAH solution, $K_4Fe^{II}(CN)_6/K_3Fe^{III}(CN)_6$ = 4 mM/1 mM redox solution, followed by development by D19 (Sample 3). Elimination of redox buffer treatment resulted in low fog density (Sample 2). When 5 mM $K_4Fe^{II}(CN)_6$ was used as a redox solution instead of $K_4Fe^{II}(CN)_6/K_3Fe^{III}(CN)_6$ = 4 mM/1 mM solution (Sample 4), fog density was 0.04 and no increase of fog density was observed.

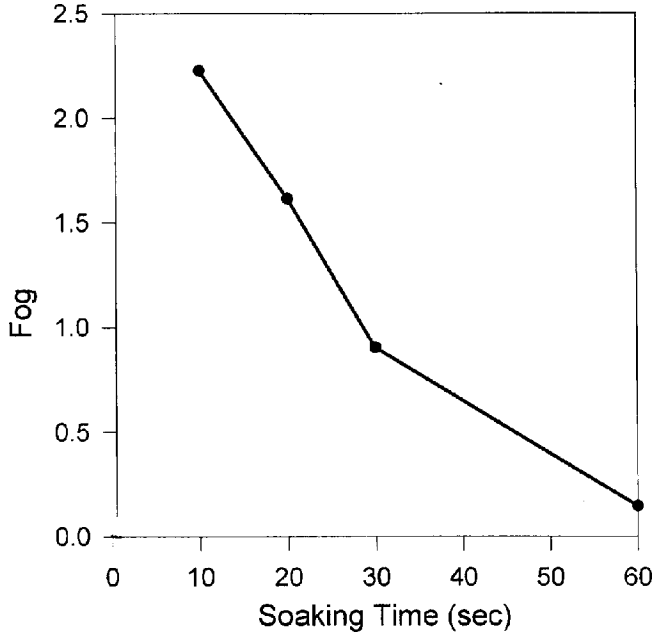

Figure 4. Dependence of fog density on soaking time in the redox buffer (AgBr emulsion).

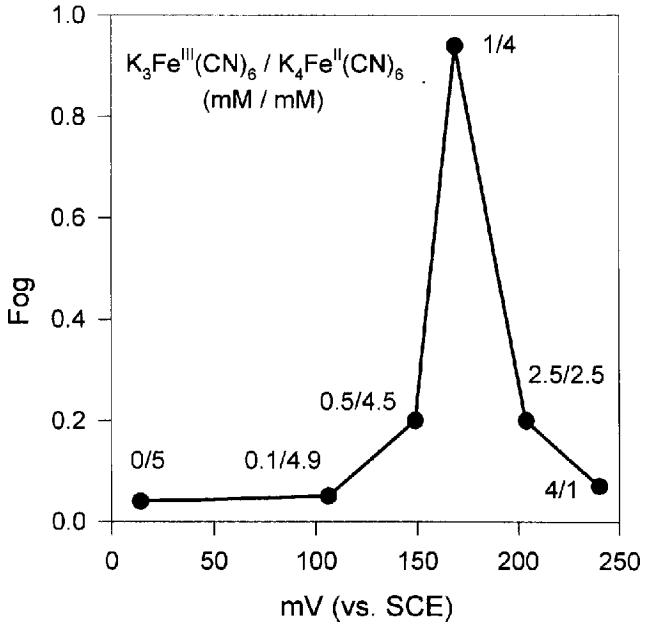

Figure 5. Effect of redox potential of the redox buffer on the fog density (AgBr emulsion).

Figure 4 shows dependence of fog density on the soaking time in the redox buffer. The standard treatment condition used for Sample 3 in Table IV was used except that the soaking time was varied. The fog density rapidly decreased with increasing soaking time.

Figure 5 shows the effect of redox potential of redox solution on fog density of an AgBr emulsion. Redox potential was varied by changing the ratio of $K_4Fe^{II}(CN)_6$ and $K_3Fe^{III}(CN)_6$. Conditions other than the ratio of $K_4Fe^{II}(CN)_6$ and $K_3Fe^{III}(CN)$ were the same as Sample 3 in Table IV. A maximum in fog density was observed. As the redox potential becomes more positive, fog density increased, reached maximum, and then decreased. Density reached maximum when the ratio of $K_4Fe^{II}(CN)_6/K_3Fe^{III}(CN)_6$ was

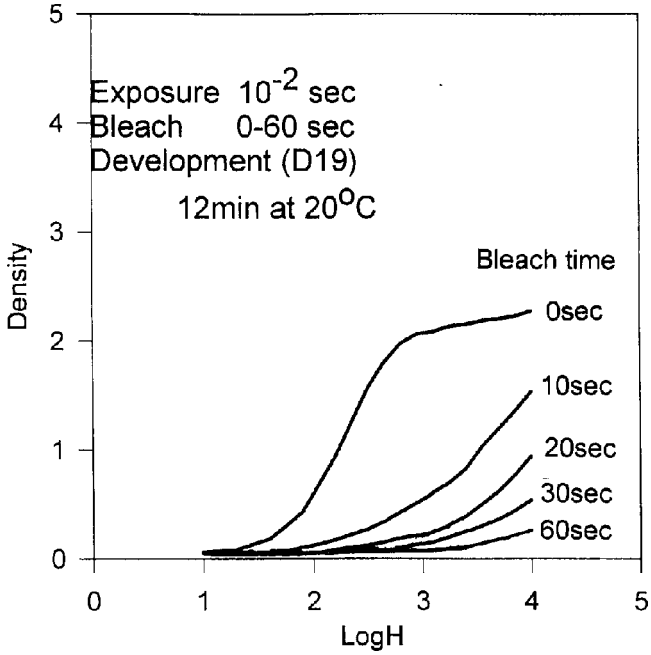

Figure 6. Bleach of the latent image by redox buffer (AgBr emulsion).

4 mM/1 mM or when the redox potential was 169 mV versus SCE.

A separate experiment was performed to examine the latent image bleach by redox solution because results shown in Figs. 3, 4, and 5 indicate that redox buffer treatment not only initiates the nucleation reaction to give fog but also depresses the nucleation reaction or bleaches the fog. To evaluate the bleaching power of the redox solution, exposed film samples were treated by redox solution before development. Unsensitized AgBr film samples were exposed as described in the sensitometry in the experimental section. The film samples were soaked in the redox solution shown in Table II for, 10, 20, 30, and 60 s, and were then developed by D19 for 12 min. Results are shown in Fig. 6. As Fig. 6 shows, density decreased with increasing soaking time in the redox buffer, showing that the latent image was bleached by redox solution.

Effect of Photographic Speed on Nucleation. Figure 7 shows the dependence of photographic speed and base plus fog on the amount of sodium thiosulfate pentahydrate added to the AgBr emulsion. With increasing amount of sodium thiosulfate, photographic speed increased, reached a maximum, and then decreased. Photographic speed was maximum when the addition level of sodium thiosulfate pentahydrate was 5.4×10^{-6} mol/mol Ag. Decrease of photographic speed by the excess amount of sodium thiosulfate is considered to be oversensitization and is significant at shorter development times. The loss of photographic speed by oversensitization decreased as development time was extended.

Figure 8 is a plot of fog density obtained by BNAH solution and redox solution treatment followed by development versus the amount of sodium thiosulfate pentahydrate used for chemical sensitization. Solutions used for the treatment were the same as those shown in Table II except that the concentration of BNAH was reduced to 1.1×10^{-5} M from 2.5×10^{-5} M. As Fig. 8 shows, dependence of nucleation fog density on sodium thiosulfate pentahydrate level was observed and was similar to that of speed on sodium thiosulfate pentahydrate level. With increasing

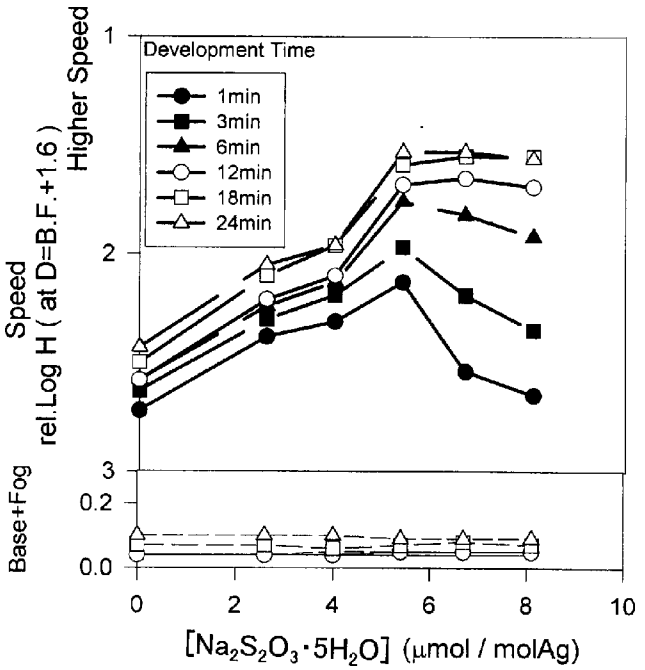

Figure 7. Effect of sulfur sensitization level on speed and base plus fog (AgBr emulsion).

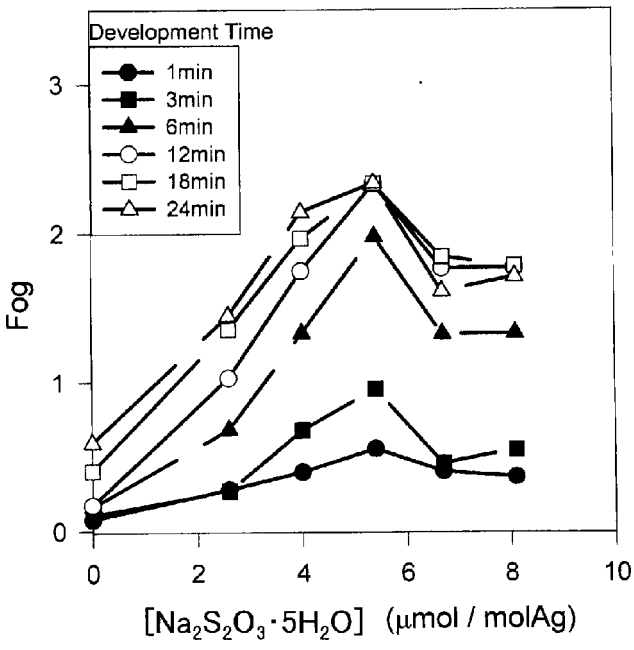

Figure 8. Effect of sulfur sensitization level on the fog density (AgBr emulsion).

addition amount of sodium thiosulfate pentahydrate, fog density increased, reached a maximum, and then decreased. Fog density, as well as the speed in Fig. 7, reached maximum when the sodium thiosulfate level was 5.4×10^{-6} mol/mol Ag. In the case of the speed shown in the Fig. 7, loss of speed by oversensitization decreased by extending the development time. However, in the case of nucleation fog shown in the Fig. 8, nucleation fog at higher levels of sodium thiosulfate pentahydrate still decreased even when the development time was 24 min.

Figure 9 shows the relationship of fog density in Fig. 8 and photographic speed in Fig. 7 for each development time. The general trend in Fig. 9 is that fog density by nucleation increases with increasing photographic speed.

Discussion

As shown in Tables III and IV, fog density did not increase when a film sample was treated by a BNAH solution followed by development, suggesting that BNAH itself does not nucleate silver halide grains. Also as shown in Tables III and IV, fog density did not increase when $Fe^{II}(CN)_6^{4-}$ was used instead of $Fe^{III}(CN)_6^{3-}$ or the mixture of $Fe^{II}(CN)_6^{4-}$ and $Fe^{III}(CN)_6^{3}$, suggesting that $Fe^{II}(CN)_6^{4-}$ does not nucleate silver halide grains. Results also suggest that $Fe^{II}(CN)_6^{4-}$ produced as a result of oxidation of BNAH by $Fe^{III}(CN)_6^{3}$ does not nucleate silver halide grains. Therefore, it is expected that the oxidation product of BNAH by $Fe^{III}(CN)_6^{3-}$ nucleated silver halide grains and made them developable.

Results in Tables III and IV indicate that $Fe^{II}(CN)_6^{4-}$ is unable to oxidize BNAH to release an active species for the nucleation. In a separate experiment, the UV absorption spectrum of a mixed solution of BNAH and $Fe^{II}(CN)_6^{4-}$ was measured in a pH 9.8 0.25 M $NaBO_2 \cdot 4H_2O$/MeOH solution. Results showed that BNAH is stable in the presence of $Fe^{II}(CN)_6^{4-}$.

It has been reported that BNAH is oxidized by $Fe^{III}(CN)_6^{3-}$ and that the oxidation reaction is retarded by $Fe^{II}(CN)_6^{4-}$ and it has been proposed that the favored oxidation process of BNAH by $Fe^{III}(CN)_6^{3-}$ is a multi-step loss of $e^- + H^+ + e^-$ (Scheme 1).[4] Scheme 1 shows that the first one-electron transfer from BNAH to $Fe^{III}(CN)_6^{3-}$ occurs, followed by deprotonation by a base, and that the second one-electron transfer from BNA• radical to $Fe^{III}(CN)_6^{3-}$ occurs. If we apply Scheme 1 to the nucleation of silver halide grains by BNAH, Scheme 2 illustrates possible reactions occurring in the fog increase by BNAH and redox buffer treatment. Reaction 1 shows the one-electron oxidation of BNAH by $Fe^{III}(CN)_6^{3-}$. Reaction 2 shows the production of the BNA• radical by deprotonation of $BNAH^{\bullet+}$. Reaction 3 shows the further oxidation of the BNA• radical by $Fe^{III}(CN)_6^{3-}$. Reaction 4 shows the nucleation of silver halide grains by the BNA• radical. Reaction 5 shows the bleach of nucleated silver halide grains by $Fe^{III}(CN)_6^{3-}$. As explained later in this section, results in this study indicate that the observed fog density by BNAH and redox solution treatment followed by development is the competitive reaction of nucleation and bleach of nucleated silver halide grains. It is also assumed from Scheme 1 that further oxidation of the active species (BNA• radical) by $Fe^{III}(CN)_6^{3-}$ is also involved.

If BNA• is produced by the oxidation of BNAH by ferricyanide as proposed by Powell,[4] it is expected[5] from the redox potential of BNA^+/ BNA• redox couple (–1.08 V versus SCE) that BNA• radical may be a possible active species for nucleation and is able to reduce silver halide grains to make them developable.

As shown in Figs. 3, 4, and 5, fog density strongly depends on the treatment conditions in the redox buffer such as treatment time, concentration of ferricyanide, or the redox potential. As shown in Fig. 3, when the concentration of $K_3Fe^{III}(CN)_6$ solution was 1.4×10^{-3} M (standard concentration), fog density decreased rapidly with increasing treatment time of $K_3Fe^{III}(CN)_6$ solution. The same trend was also observed in Fig. 4. Data in those figures indicate that the redox solution bleaches the fog centers created by the nucleation. As mentioned earlier, results in Fig. 6 show that the standard redox solution for the AgBr emulsion ($K_4Fe^{II}(CN)_6$/ $K_3Fe^{III}(CN)_6$ = 4 mM/1 mM) bleaches the latent image. Hence it is expected that the redox buffer treatment not only initiates the nucleation that leads to

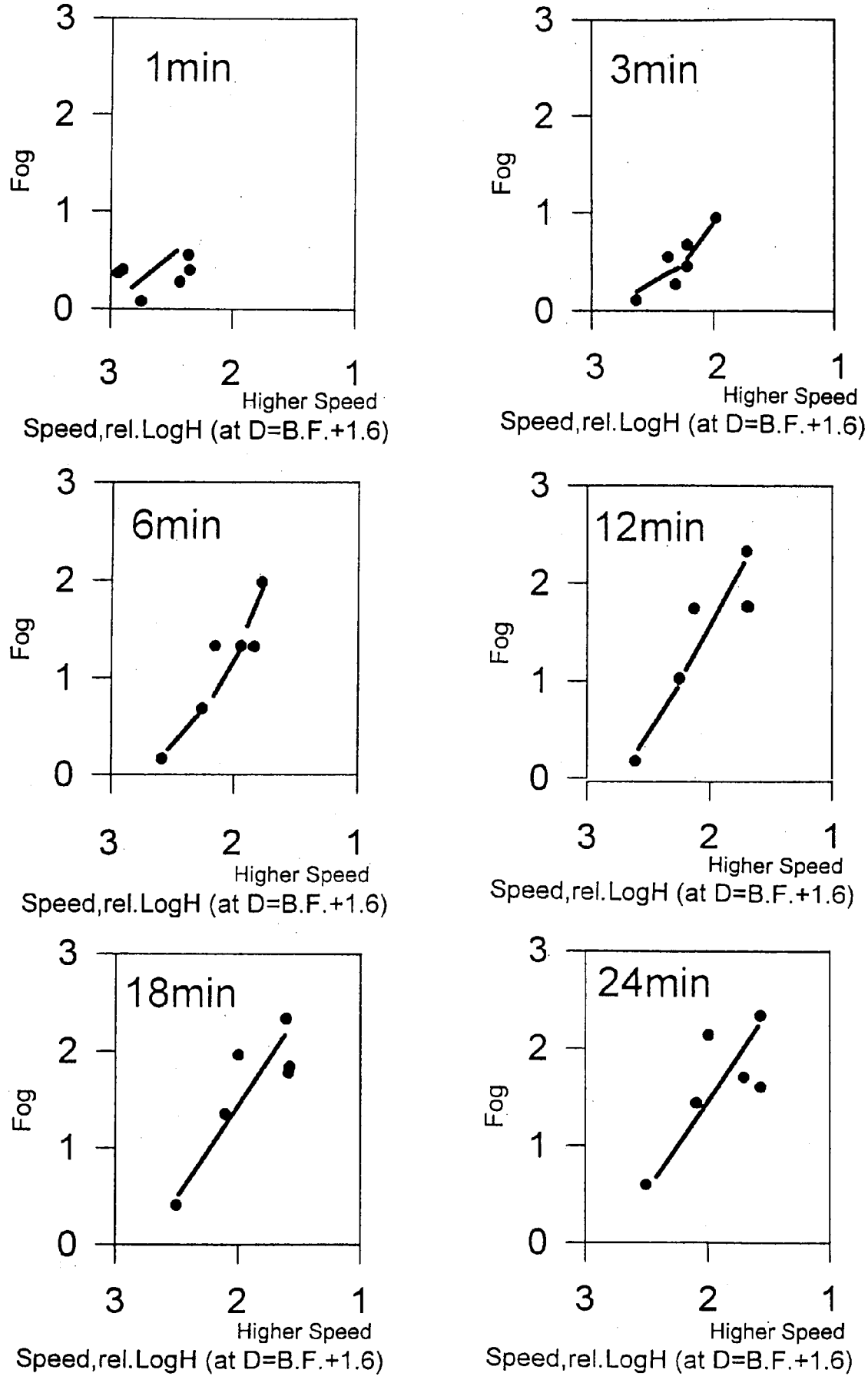

Figure 9. Correlation between speed and fog density at various development times (AgBr emulsion).

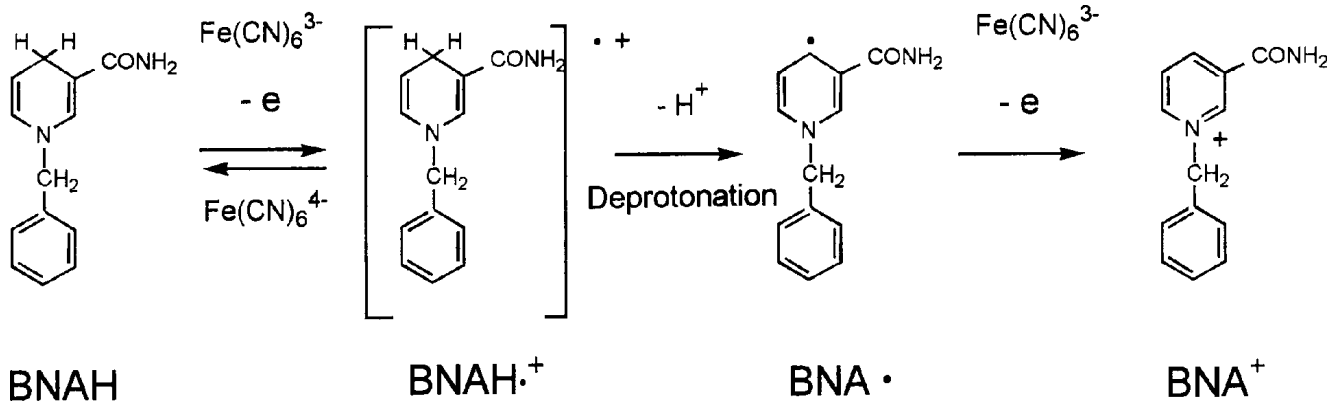

Scheme 1. Oxidation of BNAH by $K_3Fe^{III}(CN)_6$

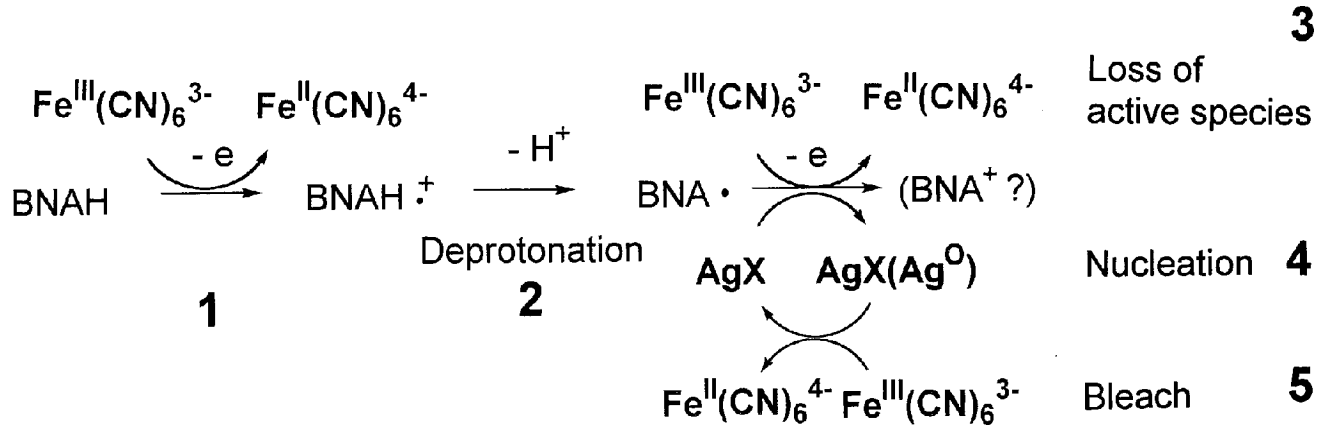

Scheme 2. Possible nucleation mechanism of silver halide grains by BNAH and $K_3Fe^{III}(CN)_6$.

the fog increase but also bleaches the fog centers created by the nucleation. In other words, a competitive reaction occurs between fog increase by nucleation and bleach of the fog.

As Fig. 3 shows, when the concentration of $K_3Fe^{III}(CN)_6$ solution was 1.4×10^{-4} M, fog density increased with increasing treatment time in $K_3Fe^{III}(CN)_6$ solution. This is probably because the bleach of the fog center is relatively slow compared to the nucleation. But, when the concentration of $K_3Fe^{III}(CN)_6$ solution was 1.4×10^{-2} M, fog density was 0.04 and no fog increase was observed. This may be because the redox solution bleached the fog centers and/or because the redox solution oxidized the active species of the nucleation so that no nucleation occurred.

The strong dependence of fog density on the redox potentials of the redox buffer shown in Fig. 5 also indicates that BNAH and redox buffer treatments involve the oxidation of the active species and/or the bleach of the fog centers. When the redox potential is more positive than the peak potential (159 mV), it is expected that the oxidation of the active species or the bleach of the fog centers becomes dominant.

As Figs. 7 and 8 show, dependence of fog density by nucleation on the sulfur sensitization level is very similar to the dependence of photographic speed on the sulfur sensitization level. Note that the nucleation fog, as well as the photographic speed, decreased when the emulsion was oversensitized. Figure 9 shows that fog density increases with increasing photographic speed of the emulsion. Direct comparison of fog density shown in Fig. 8 with photographic speed shown in Fig. 7 may not be very accurate because the fog density observed by BNAH and redox solution treatment involves not only nucleation but also bleach of nucleated silver halide grains. However, because a fairly good correlation between the photographic speed and the nucleation fog was observed, it is probably reasonable to assume that the nucleation reaction involves electron injection from the active species into the silver halide grains and that the nucleation reaction involves a similar reaction to that of the latent image formation by photoelectrons.

Conclusions

Using BNAH as a model compound of dihydropyridines, we found that the oxidation product of BNAH by ferricyanide is able to nucleate unexposed silver halide grains. The results support the proposed mechanism of the production of superhigh contrast in which dihydropyridines work as an intermediate for the nucleation.

References

1. N. Obi, Y. Kojima, and Y. Shigemitsu, *J. Imaging. Sci. Technol.* **39,** 532 (1995).
2. N. Obi, K. Suematsu, Y. Kojima, H. Muratake, and Y. Shigemitsu, *J. Imaging. Sci Technol.* **40,** 70 (1996).
3. N. Obi, J.Takeuchi, Y. Kojima, and Y. Shigemitsu, *J. Soc. Photogr. Sci. Technol. Jpn.* **60,** 228 (1997).
4. M. F. Powell, J. C. Wu, and T. C. Bruice, *J. Am. Chem. Soc.* **106,** 3850 (1984).
5. S. Fukuzumi, S. Koumitsu, K. Hironaka, and T. Tanaka, *J. Am. Chem. Sci.* **109,** 305 (1987).